Received 2 February 2018; | Revised ; | Accepted

DOI: xxx/xxxx

ARTICLE TYPE

Low-Complexity Heuristics to Beam Selection and Rate Adaptation in Sparse Massive MIMO Systems

Samuel T. Valduga*[1,3] | Luc Deneire[2] | Ramon Aparicio-Pardo[2] | André L. F. de Almeida[3] | Tarcisio F. Maciel[3] | João C. M. Mota[3]

[1]Department of Electronics and Computing - Telecommunications Engineering, UFSM, Rio Grande do Sul, Brazil
[2]Universite Côte d'Azur, CNRS, I3S, Unice, Côte d'Azur, France
[3]Department of Teleinformatics Engineering, UFC, Ceara, Brazil

Correspondence
*Email: samueltv@gtel.ufc.br

Present Address
Department of Teleinformatics Engineering, Federal University of Ceara, Campus do Pici, s/n, CP 6005 60455-970, Fortaleza, CE, Brazil.

Summary

In this work, we propose a novel formulation for a precoder design considering a practical rate assignment based on the modulation and coding scheme (MCS) of the long-term evolution (LTE) table, beam selection, and power optimization, that exploits the geometric sparsity of the multi-user (MU) massive multiple input and multiple output (MIMO) channel. We consider two different channel models, and provide an optimal solution for the joint beam selection and power optimization, as well as a heuristic using Lagrangean relaxation. Assuming knowledge of the beamspace channel, the beamspace precoder consists of selecting and optimizing the power of the beams steered to the user equipments (UEs) in order to maximize the signal-to-interference-plus-noise ratio (SINR) at the UE. Furthermore, we propose three additional simple heuristics with low-complexity. For these three heuristics, we solve the problem in two steps: i) selection of beams based on the maximal ratio transmission (MRT) principle, and ii) power allocation per UE. Simulation results show that our optimal solution can achieve a better performance than the zero forcing beamforming (ZFBF) scheme in the high sparsity cases. Besides, compared to the linear MRT precoder, the proposed low-complexity heuristics improve the performance under a scenario with channel sparsity.

KEYWORDS:
Massive MIMO, beamforming, precoding, beamspace channel representation, mixed integer linear programming (MILP), Lagrangean relaxation, sum rate.

1 | INTRODUCTION

Massive multiple input and multiple output (MIMO) is one of the key technologies for the 5th generation (5G) wireless communication systems due to its potential to achieve high data rates and its robustness against interference, fading, hardware imperfections and failure[1]. In his seminal paper, Marzetta[2] showed that when the number of antennas grows very large, the effect of additive noise decreases, as well as the required transmitted energy per bit.

Massive MIMO systems have the potential to achieve high data rates mainly when more user equipments (UEs) are allocated the same frequency resource. Under the multi-user (MU) perspective, the systems have a huge potential to decrease power consumption and to improve the communication system performance[3]. However, when the number of base station (BS) antennas is moderate, intra-cell interference among UEs appears and has to be effectively handled. Transmit beamforming is one of the techniques that achieves enhanced performance in MU massive MIMO systems, determining the complex antenna gains that optimize some performance criterion, e.g., sum rate. In the literature[3], transmit beamforming

structures have been analyzed. In particular, they show that optimal beamforming can be seen as a tradeoff between maximal ratio transmission (MRT), which is optimal in the absence of interference, and zero forcing beamforming (ZFBF), that cancels the multi-user interference (MUI). In this latter case[3], the ZFBF implies a significant computational complexity compared to MRT.

Classical beamforming[4] is defined as a single steering vector of interest where the aim is to ensure that of inner product between beamforming weight vector and the steering vectors of interest is large, whereas the inner product of the beamforming weight vector and all other steering vectors is small, i.e., to mitigate interference. It is applied to both receive beamforming and unicast transmit beamforming for a single receiver. For MU transmit beamforming in the downlink case, when the transmitter has multiple antennas, multiple transmit beamforming weight vectors are designed to carry different cochannel unicast transmissions, each meant to reach the receiver of a different UE. These vectors are created to balance the interference between different transmissions. This concept was introduced in the literature[5], where some downlink beamforming techniques have been developed. In some previous work[6], convex optimization methods are introduced to solve the problem.

Along the last years, several works have investigated precoding schemes[7,8,9,10,11]. The sparsity property of the MU channel matrix could be exploited to obtain a sparse approximate inverse[7]. However, this kind of scheme still requires many operations to compute a matrix inverse. A way to lower complexity is proposed by Sun et.al.[8], where the authors propose a beam domain multiple access (BDMA) transmission scheme in which MU are served by different beams. These beams are the eigenvectors of the channel matrix. The BDMA algorithm exploits the channel coupling matrices of a stochastic MIMO channel model[12]. When considering the so-called virtual channel[13], the matrices collecting the eigenvectors are discrete Fourier transforms (DFT) matrices. In this case, the beams are fixed and do not depend on the channel. Although BDMA is near optimal, it does not consider the sparsity of the beam domain channel and does not allow to schedule more than one UE per transmitting beam.

Yu et. al. proposed a low-complexity transceiver design[9], namely semi-random beam pairing (SRBP), for sparse multipath massive MIMO channels[13]. The idea is to transmit simultaneous data streams, and in the end, to decouple them using successive interference cancellation (SIC). However, it is well known that SIC can propagate errors, mainly if the number of streams is large.

In the search for low complexity solutions, Li et. al. proposed a precoder design[10], based on the maximization of the minimum signal-to-interference-plus-noise ratios (SINRs) perceived by all MU, under an equal quality of service (QoS) constraint. This max-min formulation leads to a quasi-convex optimization problem that can be solved by a low complexity algorithm based on relaxation techniques. One way to achieve maximum sum rate in a practical scenario is considering to jointly optimize modulation and coding schemes (MCSs) and transmit beamforming[11]. In these approaches, the rate adaptation consists in assigning MCSs for MUs (for example, according to the 3GPP long-term evolution (LTE) table[14], c.f., Chap. 5). In general, this formulation leads to a mixed integer linear programming (MILP) problem. In most cases, it is impractical due to its high computational complexity.

Recent studies have demonstrated that, as the spatial dimension increases, the physical MIMO channels exhibit poor scattering[15,16,17,18]. This is the case in macro-cell urban environments, where the propagation links between the BS and UE are often blocked by large buildings or when clusters of multipaths are shared by the same MUs[19,20,7,21].

In this paper, we propose low-complexity heuristics to beam selection and rate adaptation in sparse massive MIMO system. The main contributions are summarized as follows:

- We propose a precoder design considering a practical rate assignment (based on the MCS of the LTE table), beam selection, and power optimization that exploits the geometric sparsity of the MU massive MIMO channel using its beamspace representation. We show an optimal solution to capacity (sum rate) following the MRT principle combined with beam selection, called MRT with selection.

- We design a new heuristic to simplify the beam selection and power optimization procedure based on Lagrangean relaxation[22].

- We show that, for a sparse channel, performance improvements can be achieved by selecting the proper beams followed by MRT beamforming on these beams. In the end, we propose three additional simple heuristics with low-complexity to beam selection in the beamspace domain. For these heuristics, we solve the problem in two steps: i) selection of beams based on the MRT, ii) power allocation per UE. The first heuristic uses MRT as an initial point and removes beams whose removal increases the SINR. The second heuristic sequentially assigns single beams to UEs using a sub-optimal solution provided by the Munkres algorithm[23]. The third heuristic takes the previous heuristic as an initial point, then allocates more beams, provided that this allocation improves the SINR. We show that adding and/or removing some beams improves the system performance. Simulation results show that our optimal solution can achieve a better performance than the ZFBF scheme

for high sparsity cases. Besides, compared to the linear MRT precoder, the proposed low-complexity heuristics improve the performance under a scenario with channel sparsity.

In our previous work[24], we proposed three low-complexity heuristics and evaluate them in a sparse channel scenario. In this work, we extend the MRT with selection for a practical scenario using MCS. We provide an optimal solution, and a heuristic for decreasing the complexity. Also, the MRT with selection is evaluated under two channel model representations.

The rest of this paper is organized as follows. Section 2 presents the system model and the main assumptions. Section 3 presents the problem formulation and the proposed heuristics. In Section 5, simulations results are shown. Finally, Section 6 brings some concluding remarks and perspectives.

Notations: normal letters represent scalar quantities while boldface lower-case and boldface upper-case letters indicate vectors and matrices, respectively. Superscripts '$(\cdot)^T$', and '$(\cdot)^H$' represent the transpose and the conjugate transpose operations, respectively. $\mathbf{I}_N$ denotes an $N \times N$ identity matrix. Frobenius norm is denoted by $\|\cdot\|_{\mathrm{F}}$, while $\odot$ and $\otimes$ respectively denote the Hadamard and Kronecker products.

2 | SYSTEM MODEL AND ASSUMPTIONS

In this section, we introduce the system model and some general assumptions for two different channel models based on the beam domain channel representation. Furthermore, we address the beam selection problem.

2.1 | General Definitions

Consider a downlink scenario composed of a single massive MIMO BS with M_T transmit antennas and K UEs, each one being equipped with a single antenna. We assume that all UEs share the same time-frequency resource and that the BS has the knowledge of the channel. We model the received signal y_k, with $k \in \{1, \dots, K\}$, at the k^{th} UE as:

$$y_k = \mathbf{h}_k^H \left(\mathbf{w}_k x_k + \sum_{i \neq k}^{K} \mathbf{w}_i x_i \right) + n_k, \tag{1a}$$

$$= \mathbf{h}_k^H \mathbf{W} \mathbf{x} + n_k, \quad k \in \{1, \dots, K\}, \tag{1b}$$

where n_k represents the additive noise at the receive antenna, which is complex Gaussian with zero mean and variance σ_k^2; $\mathbf{h}_k \in \mathbb{C}^{M_T \times 1}$ is the multiple input and single output (MISO) channel, and $\mathbf{w}_k \in \mathbb{C}^{M_T \times 1}$ is the k^{th} UE precoder.

Writing the emitted symbol vector as $\mathbf{x} = \begin{bmatrix} x_1 & \dots & x_K \end{bmatrix}^T$, the precoder matrix $\mathbf{W}$ is given by $\mathbf{W} = \begin{bmatrix} \mathbf{w}_1 & \dots & \mathbf{w}_K \end{bmatrix} \in \mathbb{C}^{M_T \times K}$ as in (1b). The global received signal taking into account all UEs is given by:

$$\mathbf{y} = \begin{bmatrix} y_1 & \dots & y_K \end{bmatrix}^T = \mathbf{H}^H \mathbf{W} \mathbf{x} + \mathbf{n}, \tag{2}$$

where $\mathbf{n} = \begin{bmatrix} n_1 & \dots & n_K \end{bmatrix}^T \in \mathbb{C}^{K \times 1}$ is the global noise vector, and $\mathbf{H} = \begin{bmatrix} \mathbf{h}_1 & \dots & \mathbf{h}_K \end{bmatrix} \in \mathbb{C}^{M_T \times K}$ is the channel matrix.

Following the literature[25,26], the so-called virtual channel representation is written as:

$$\mathbf{h}_k = \mathbf{A}_T \mathbf{g}_k \in \mathbb{C}^{M_T \times 1}, \tag{3}$$

where $\mathbf{g}_k \in \mathbb{C}^{M_T \times 1}$ is the beam domain channel vector of the virtual channel, $\mathbf{A}_T \in \mathbb{C}^{M_T \times M_T}$ is the array steering matrix given by

$$\mathbf{A}_T = \begin{bmatrix} \mathbf{a}_T(\theta_0) & \dots & \mathbf{a}_T(\theta_{M_T - 1}) \end{bmatrix} \in \mathbb{C}^{M_T \times M_T}, \tag{4}$$

which can be set up as a DFT matrix, and the array steering vector is given by:

$$\mathbf{a}_T(\theta) = \frac{1}{\sqrt{M_T}} \begin{bmatrix} 1 & e^{-j2\pi\theta} & \dots & e^{-j2\pi\theta(M_T - 1)} \end{bmatrix}^T.$$

where $\theta = d \frac{\sin(\phi)}{\lambda}$ is the azimuth spatial frequency, d is the antenna spacing and λ is the wavelength. The angle ϕ measures the angle between the impinging ray and the normal to the array.

Note that we assume the same array steering matrix $\mathbf{A}_T$ for all UEs. This assumption reduces the complexity of the model and it is known that the channel for each UE can be represented using the same basis when M_T is sufficiently large[8,27,28,16].

Following some previous works[29,17], the extension for a rectangular uniform planar array (UPA) using the same DFT matrix for all UEs can be done. However, a Kronecker product is used to represent the azimuth and elevation spatial frequencies in two dimensional arrays[17]. Furthermore, the array structure does not affect the precoder design (based on beam selection). Consequently, other bases and array structures can be used to represent the channel.

Rewriting (1) with (3), we obtain:

$$y_k = \mathbf{g}_k^H \mathbf{A}_T^H \mathbf{w}_k x_k + \mathbf{g}_k^H \mathbf{A}_T^H \sum_{i \neq k}^{K} \left(\mathbf{w}_i x_i \right) + n_k, \tag{5}$$

so that the received signal for all UEs can be written as follows:

$$\mathbf{y} = \mathbf{G}^H \mathbf{A}_T^H \mathbf{W} \mathbf{x} + \mathbf{n}, \tag{6}$$

where $\mathbf{G} = \begin{bmatrix} \mathbf{g}_1 & \dots & \mathbf{g}_K \end{bmatrix} \in \mathbb{C}^{M_T \times K}$. Considering unit-power uncorrelated symbols ($\mathbb{E}\left\{ \mathbf{x}\mathbf{x}^H \right\} = \mathbf{I}_K$) the SINR_k at the k-th UE can be expressed as:

$$\mathrm{SINR}_k = \frac{\left| \mathbf{h}_k^H \mathbf{w}_k \right|^2}{\sum_{i \neq k}^{K} \left| \mathbf{h}_k^H \mathbf{w}_i \right|^2 + \sigma_k^2}. \tag{7}$$

2.2 | Independent and Identically Distributed Beam Domain Channel Model

Consider $\mathbf{G}$ generated as:

$$\mathbf{G} = \mathbf{\Sigma} \odot \tilde{\mathbf{G}}, \quad \text{with} \quad \tilde{\mathbf{G}} \approx \mathcal{CN}(0,1), \tag{8}$$

where $\odot$ is the Hadamard product. The sparsity of the channel model is described by the matrix $\mathbf{\Sigma} \in M_T \times K$ whose elements are independent identically distributed (i.i.d.) Bernoulli random distributed of parameter κ. The sparsity level is the average number of zero elements of $\mathbf{\Sigma}$ and is equals $\chi = 1 - \kappa$. The non-zero entries of $\mathbf{g}_k$ can be modeled as Bernoulli random variables [26]. Since the distances between the UE and the BS are larger than the distance between the antennas, the assumption of equal probability of a non-vanishing path for each UE is reasonable. When the number of antennas increases to a massive number, the channel composed by a low number of scatterers tends to be sparse in the beam domain due to the fact that resolvable paths contribute less [15]. Thereby, the sparse massive channel is well represented using the virtual channel model.

The parameter χ is introduced to describe the sparsity of the channel, and this is defined as the non-zero probability of entries in the distinct virtual channel matrix. Following some previous work [26], the entries of $\mathbf{G}$ are defined as random variables taking values from a complex normal distribution $\mathcal{CN}(0,1)$, i.e., the entries in the sparse virtual channel matrix under the above i.i.d. assumption follows the Gaussian-Bernoulli distribution.

2.3 | Geometric-Stochastic Beam Domain Channel Model

Following the literature [17,18], in some scenarios (e.g., in mmWave) the multipaths are expected to form a sparse set of single-bounce components. In this context, the poor scattering effects can result in the virtual angular domain with a sparse channel matrix representation [16,21]. The non-zero coefficients are related to the approximately disjoint subsets of paths and are modeled as independent complex Gaussian random variables. The number of non-zero entries on $\mathbf{G}$ defines a fixed number of beams simultaneously used at the BS, and this quantity depends on the sparsity level. Thereby, $\mathbf{G}$ is sparse with level equals χ and most of the power is concentrated in a few dominant entries.

Then, $\mathbf{g}_k$ can be modeled as:

$$\mathbf{g}_k = \mathbf{A}_T^H \mathbf{h}_k, \tag{9}$$

$$\mathbf{h}_k = \sum_{p=1}^{L} \beta_{k,p} \mathbf{a}_T(\theta_{k,p}), \tag{10}$$

where L is the number of scatterers (c.f. Fig. 1); $\mathbf{a}_T(\theta_{k,p})$ represents the steering vector with $\theta \in [-\pi, \pi]$ and β represents the complex gain of path p, which follows a $\mathcal{CN}(0,1)$ distribution. Furthermore, following the literature [18], we assume that the smallest elements in $\mathbf{g}_k$ can be neglected.

2.4 | Beam Selection

Considering the previous beam channel discussion in the last subsections, let us define the selection vector as:

$$\mathbf{s}_k = \begin{bmatrix} s_{1,k} & \dots & s_{M_T,k} \end{bmatrix}^T, \tag{11}$$

where $s_{t,k} \in \{0,1\}$ defines the selection of transmit beam t for user k. However, in a more general case, $s_{t,k}$ may actually be considered as a "gain" and be a complex scalar. Then, the beamformer can be written as:

$$\begin{aligned} \mathbf{w}_k &= s_{t,k} \cdot \mathbf{a}_T(\theta) \\ &= s_{t,k} \cdot \frac{1}{\sqrt{M_T}} \begin{bmatrix} 1 & e^{-j2\pi \cdot \theta_{M_T}} & \dots & e^{-j2\pi(M_T-1)\theta_{M_T}} \end{bmatrix}^T \\ &= \sum_{t=0}^{M_T-1} s_{t,k} \mathbf{a}_T \left(\frac{t}{M_T - 1} \right) = \mathbf{A}_T^T \mathbf{s}_k = \mathbf{A}_T \mathbf{s}_k. \end{aligned} \tag{12}$$

Hence, the received signal in (1) can be rewritten as:

$$\begin{aligned} y_k &= \mathbf{h}_k^H \left(\mathbf{w}_k x_k + \sum_{i \neq k}^{K} \mathbf{w}_i x_i \right) + n_k, \\ &= \mathbf{g}_k^H \mathbf{A}_T^H \left(\mathbf{A}_T \mathbf{s}_k x_k + \sum_{i \neq k}^{K} \mathbf{A}_T \mathbf{s}_i x_i \right) + n_k, \\ &= \mathbf{g}_k^H \left(\mathbf{s}_k x_k + \sum_{i \neq k}^{K} \mathbf{s}_i x_i \right) + n_k, \\ &= \mathbf{g}_k^H \mathbf{S}\mathbf{x} + n_k \quad \forall k, \end{aligned} \tag{13}$$

where $\mathbf{S} = \begin{bmatrix} \mathbf{s}_1 & \dots & \mathbf{s}_K \end{bmatrix}$. The complete signal (2), can then be rewritten as:

$$\mathbf{y} = \mathbf{G}^H \mathbf{S}\mathbf{x} + \mathbf{n}, \tag{14}$$

where the beam domain channel matrix can be expressed as $\mathbf{G} = \begin{bmatrix} \mathbf{g}_1 & \dots & \mathbf{g}_K \end{bmatrix}$.

To exemplify an application scenario, we could assume a low-number of scatterers, where $L \ll M_T$, some overlapped angles of departure (AoDs), and shared scatterers among UEs depending on the cluster distribution [21] (see Figure 1). Then paths between BS and the UE are highly correlated. It is a result of a small angular spread of the outgoing rays at the BS.

For instance, consider two simple cases following the virtual channel model with six uniformly spaced virtual angles (six transmit antennas), three UEs and three multipath clusters. Remember that in this model, the path gain of each UE is linked to the DFT matrix, describing the AoDs. For simplicity, consider one to represent the complex path gains, and zero otherwise. Regarding the virtual channel model, this scenario

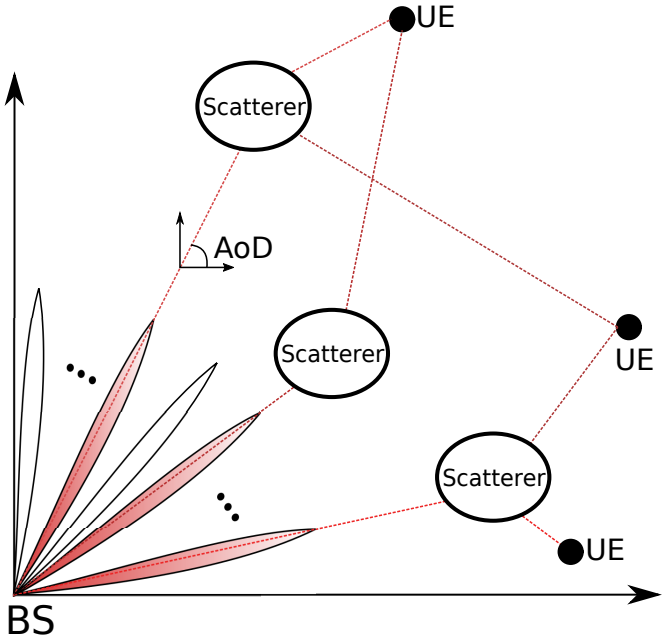

FIGURE 1 Illustration of a scenario with a low-number of the scatterers. Note that some scatterers share the same transmit beam.

has the following structure:

$$\mathbf{G}^H = \begin{bmatrix} 1\,0\,0\,0\,0\,1 \\ 0\,0\,0\,1\,0\,0 \\ 0\,0\,1\,0\,0\,0 \end{bmatrix}.$$

In this interference-free case, there in no interference since $\mathbf{G}^H$ has no nonzero elements in the same columns. Furthermore, the sparsity level is measured by the ratio of zero elements of $\mathbf{G}^H$ over the total number of elements KM_T, $\chi = 1 - (4/(3 \cdot 6) = 1 - 0.222) \approx 78\%$. Consider a second example with:

$$\mathbf{G}^H = \begin{bmatrix} 1\,0\,0\,0\,0\,1 \\ 0\,0\,1\,1\,0\,0 \\ 1\,0\,1\,0\,0\,0 \end{bmatrix}.$$

Notice that interference exist since $\mathbf{G}^H$ has more than one nonzero element in a columns 1 and 3. In this example, the sparsity level is $\chi = 1 - 6/(3 \cdot 6) = 1 - 0.333 \approx 67\%$.

3 | PROBLEM FORMULATION

In the classical MIMO formulation, transmit beamforming (or precoding) can be optimized to maximize some performance utility metric, which is generally a function of the SINR of the active UEs[30,3]. In general, two approaches can be taken: i) to optimize a performance criterion for given transmit power constraints or ii) to minimize the total transmit power under given SINR constraints. The first approach assumes the following transmit power constraint:

$$\text{tr}\left(\mathbf{W}^H\mathbf{W}\right) = \sum_{k=1}^{K} \|\mathbf{w}_k\|_2^2 = P = \sum_{k=1}^{K} P_k.$$

Considering a per UE power constraint, the optimization problem can be expressed as

$$\begin{aligned} &\max_{\mathbf{w}_1,\ldots,\mathbf{w}_K} f(\text{SINR}_1, \ldots, \text{SINR}_K) \\ &\text{s.t. } \|\mathbf{w}_k\|_2^2 = P_k, \qquad \forall k \in \{1, \ldots, K\}. \end{aligned} \tag{15}$$

where $f(\text{SINR}_1, \ldots, \text{SINR}_K)$ is some suitable function of the SINRs and P_k is the power allocated to the k^{th} UE. A possible performance criterion is the sum rate:

$$\text{sum rate} = \sum_{k=1}^{K} \log_2(1 + \text{SINR}_k). \tag{16}$$

The second optimization problem consists in minimizing the total transmit power which can be formulated as:

$$\begin{aligned} &\min_{\mathbf{w}_1,\ldots,\mathbf{w}_K} \sum_{k=1}^{K} \|\mathbf{w}_k\|_2^2, \\ &\text{s.t. } \text{SINR}_k = \gamma_k. \end{aligned} \tag{17}$$

The parameters γ_k are the SINRs that each UE shall be granted at the optimum of (17), using as little transmit power as possible. The γ-parameters can, for example, describe the SINR required to achieve certain data rates. However, the optimization of UE transmit beamforming is generally a nondeterministic polynomial-time (NP) hard problem[4,31,3].

Classical precoders can be easily expressed in the beam domain such as the MRT, where the performance (sum rate) is limited due to MUI[32]. This MUI can be avoided thanks to ZFBF[30,33,7], at the cost of some computational complexity (due to the number of operations required to compute the pseudo-inverse $\mathcal{O}(K^2 M_T^2)$). Moreover, these beamformers use full (instantaneous) channel knowledge, which asks for large channel state information (CSI) feedback to the BS[34]. To alleviate this feedback load, it is possible to transmit only on one beam. Hence, only second order statistics are needed, which are long-term parameters that vary slowly compared to the instantaneous channel coefficients or path gains[12,8]. Using only the beam gain knowledge from the channel covariance matrix, Sun et. al. proposed to select a single beam using the maximum beam gain[8]. However, this limits the performance (rate) per UE.

4 | PROPOSED SOLUTION

In this section, we propose a precoder design considering a practical rate assignment (based on MCS, c.f. Table 1), beam selection, and power optimization per beam that assumes the

beam domain channel model for massive MIMO (c.f., (8) and (10)). We design a new heuristic to simplify the beam selection and power optimization procedure based on Lagrangean relaxation[22]. Furthermore, for completeness we briefly describe three other simple low-complexity heuristics[24].

4.1 | General Definitions

Firstly, because $\mathbf{g}_k$ is named beam domain channel, we call $\mathbf{s}_k$ the virtual beamformer or virtual precoder, since (14) and (2) have the same form. Based on this, we rewrite the classical beamforming problem as a "virtual beamforming" problem.

The SINR in (7) can be expressed in terms of $\mathbf{g}_k$ and $\mathbf{s}_k$ as:

$$\text{SINR}_k = \frac{\left|\mathbf{g}_k^H \mathbf{s}_k\right|^2}{\sum\limits_{i\neq k}^{K} \left|\mathbf{g}_k^H \mathbf{s}_i\right|^2 + \sigma_k^2}. \tag{18}$$

The useful signal power is $\mathbf{g}_k^H \mathbf{s}_k \mathbf{s}_k^H \mathbf{g}_k = \left|\mathbf{g}_k^H \mathbf{s}_k\right|^2$, whereas the interference power is $\sum_{i\neq k} \left|\mathbf{g}_k^H \mathbf{s}_i\right|^2$. Thus, minimizing the MUI boils down to:

$$\begin{aligned} &\min \sum_k \sum_{i\neq k} \left|\mathbf{g}_k^H \mathbf{s}_i\right|^2, \\ &\text{s.t. } \left\|\mathbf{s}_k\right\|_2^2 = P_k. \end{aligned} \tag{19}$$

Starting from (19), we can minimize the overall interference (over all UEs k)[35,36,37]. Noting that $\left|\mathbf{g}_k \mathbf{s}_k\right|^2$ is a constant, minimizing $\sum_k \sum_{i\neq k} \left|\mathbf{g}_k^H \mathbf{s}_i\right|^2$ is equivalent to minimizing $\sum_k^K \sum_i^K \left|\mathbf{g}_k^H \mathbf{s}_i\right|^2$ and the MUI minimization problem can be rewritten as:

$$\begin{aligned} &\min \sum_i \sum_k \left|\mathbf{g}_k^H \mathbf{s}_i\right|^2 \\ &\text{s.t. } \left\|\mathbf{s}_k\right\|_2^2 = P_k, \quad \forall k, \end{aligned} \tag{20}$$

where $\min \sum_i \sum_k \left|\mathbf{g}_k^H \mathbf{s}_i\right|^2 = \min \left\|\mathbf{G}^H \mathbf{S}\right\|_{\text{F}}^2$.

4.2 | Optimal Solution via Beam Selection, Power Beam Optimization and Rate Assignment: A MILP Formulation

In this subsection, the aim is to find an optimal solution to the performance achieved by beam selection using integer linear programming (ILP) and MRT with selection. The problem is mainly to find a feasible set of beams such that MRT on these beams delivers optimal performance. Moreover, we write the problem to maximize the sum rate using a set of discrete rates[11,38], supported by a set of beam gains. For instance, in the practical cellular communication systems such as LTE, the rate of each UE takes discrete rate values determined by specific MCSs assigned to each UE. Corresponding to each MCS and rate, a minimum received γ level is required. See Table 1 for more details.

The rate of the k^{th} UE from the associated γ could be obtained by applying the Shannon capacity formula: $\log_2(1+\gamma_k)$. However, these values are continuous and should be discretized according to some criterion. In the simulations section, we will discuss the discretization[1]. Due to this limitation, this paper assumes that the Table 1 is a good point to start. Let us express the rates δ as a set Δ, and γ_k as the γ achieved by index υ. We assume that the *binary* variables s represent the selected beam and q the rate assignment, as follows:

$$s_{t,k} = \begin{cases} 1, & \text{if the } t^{th} \text{ beam is assigned to the } k^{th} \text{ UE,} \\ 0, & \text{otherwise.} \end{cases}$$

$$q_{k,\upsilon} = \begin{cases} 1, & \text{if the } k^{th} \text{ UE is using only the rate } \delta_\upsilon, \\ 0, & \text{otherwise.} \end{cases}$$

The υ index corresponds to the rate in the set $\Delta = \{\delta_1, \ldots, \delta_\upsilon\}$ as defined in Table 1 (c.f., $\log_2(1+\gamma_k) = \delta_\upsilon$ for all $\gamma_{\upsilon-1} \leq \gamma_k < \gamma_\upsilon$, and $\upsilon \geq 1$).

We consider a constraint on the maximum tolerable level of MUI[39], termed hereafter limited multi-user interference (LMUI)[2]. Thereby, the SINR in (7) can be expressed in terms of the LMUI as:

$$\text{SINR}_k = \frac{\left|\mathbf{g}_k^H \mathbf{w}_k\right|^2}{\text{LMUI} + \sigma_k^2}. \tag{21}$$

The SINR considering a minimal γ requirement for each UE can be formulated as follows:

$$\text{SINR}_k \geq \sum_{\upsilon\in\Delta} \gamma_k q_{k,\upsilon}, \tag{22}$$

where γ_k represents the minimum SINR. Note that the constraint (22) is non-convex, even if the binary variables are relaxed to be continuous variables taking values in [0, 1]. Using (21), we get an equivalent inequality as an alternative to (22), as follows:

$$\left|\mathbf{g}_k^H \mathbf{w}_k\right|^2 \geq \sum_{\upsilon\in\Delta} \gamma_k q_{k,\upsilon} A, \tag{23}$$

where $A = \text{LMUI} + \sigma_k^2$ and $\mathbf{w}_k$ is the precoder for each k.

Our goal is to maximize the sum rate. Thus, the objective function can be written as:

$$\max_{q,s} \sum_k \sum_\upsilon \delta_\upsilon q_{k,\upsilon}, \tag{24}$$

where $\sum_k \sum_\upsilon \delta_\upsilon q_{k,\upsilon}$ represents the downlink sum rate with discretized rate values.

[1]Determination of the optimal values is out of scope of this paper.

[2]This limit is required for supporting a MCS and it is based on control of the temperature-interference between primary and secondary UEs into cognitive radio system.

TABLE 1 Data rates and minimum received γ requirements of LTE systems [14,11].

Index	υ	0	1	2	3	4	5	6	7	8	9	10	11	12	13	14	15
Data Rate	δ	0	0.1523	0.2344	0.3770	0.6010	0.8770	1.1758	1.4766	1.9141	2.4063	2.7305	3.3223	3.9023	4.5234	5.1152	5.5574
SINR Level (dB)	γ	0	-9.478	-6.658	-4.0898	-1.798	0.3999	2.424	4.489	6.367	8.456	10.266	12.218	14.122	15.849	17.786	19.809

We must ensure that each UE chooses only one rate [11] as follows:

$$\sum_{\upsilon\in\Delta} q_{k,\upsilon} \leq 1, \forall k. \tag{25}$$

Then, (25) is a constraint on the binary variables for the k^{th} UE to be served with only one rate, i.e., $\sum_{\upsilon\in\Delta} q_{k,\upsilon} = 1$, or the k^{th} UE be not served, which implies $\sum_{\upsilon\in\Delta} q_{k,\upsilon} = 0$.

Therefore, considering (23), (24) and (25), the problem for selecting beams and discrete rates for multiple UE can be expressed as a binary integer linear programming (BILP) problem, as follows:

$$\max_{q,s} \sum_{k}\sum_{\upsilon} \delta_\upsilon q_{k,\upsilon} \tag{26a}$$

$$\text{s.t.} \sum_{\upsilon\in\Delta} \gamma_{k,\upsilon} q_{k,\upsilon} A_k - \left|\mathbf{g}_k^H(\mathbf{w}_k \odot \mathbf{s}_k)\right|^2 \leq 0, \quad \forall k \tag{26b}$$

$$\sum_{\upsilon\in\Delta} q_{k,\upsilon} \leq 1, \forall k \tag{26c}$$

$$\sum_{i\neq k}^{K} \left|\mathbf{g}_k^H(\mathbf{w}_i \odot \mathbf{s}_i)\right|^2 \leq \text{LMUI}, \quad \forall k \tag{26d}$$

$$s_{t,k} \in \{0,1\}, \quad \forall k \tag{26e}$$

$$q_{k,\upsilon} \in \{0,1\}, \quad \forall k. \tag{26f}$$

The formulation consists in selecting discrete rates and beam gains such that the sum rate is maximized for a given LMUI level. Notice that, in this proposal, the problem is to maximize the sum rate of all UEs, assuming each achievable rate δ_υ is chosen from a predefined discrete rate set Δ.

Furthermore, in our proposal, we assume that the precoder $\mathbf{w} = \mathbf{g}$, where we aim to maximize the MRT with selection. Then, (26) can be written as:

$$\max_{q,s} \sum_{k}\sum_{\upsilon} \delta_\upsilon q_{k,\upsilon} \tag{27a}$$

$$\text{s.t.} \sum_{\upsilon\in\Delta} \gamma_{k,\upsilon} q_{k,\upsilon} A_k - \left|\mathbf{g}_k^H(\mathbf{g}_k \odot \mathbf{s}_k)\right|^2 \leq 0, \quad \forall k \tag{27b}$$

$$\sum_{\upsilon\in\Delta} q_{k,\upsilon} \leq 1, \forall k \tag{27c}$$

$$\sum_{i\neq k}^{K} \left|\mathbf{g}_k^H(\mathbf{g}_i \odot \mathbf{s}_i)\right|^2 \leq \text{LMUI}, \quad \forall k \tag{27d}$$

$$s_{t,k} \in \{0,1\}, \quad \forall k \tag{27e}$$

$$q_{k,\upsilon} \in \{0,1\}, \quad \forall k. \tag{27f}$$

Note that the problem in (27) is not assuming power constraints. As long as, the beams ($\mathbf{g}_k$) do not change with the power, the variables $s, q \in \{0,1\}$ select the rates and beams, respectively. Thereby, the problem should be solved in two steps. First, it selects beam gains and rates and afterwards it optimizes the power. However, the optimal solution on performance is not achieved because the power optimization is made in a second step and per UEs. Moreover, optimally solving a BILP problem can lead to high computational complexity [40]. We discuss the complexity analysis in Section 5.2.

Since the difficulty of solving the ILP is restricting a solution to binary values, this problem could be relaxed in parts. It means that the binary selection in the beams (s) can be relaxed to positive continue values s'. Therefore, this problem is expressed as a MILP formulation:

$$\max_{q,s} \sum_{k}\sum_{\upsilon} \delta_\upsilon q_{k,\upsilon} \tag{28a}$$

$$\text{s.t.} \sum_{\upsilon\in\Delta} \gamma_{k,\upsilon} q_{k,\upsilon} A_k - \left|\mathbf{g}_k^H(\mathbf{g}_k \odot \mathbf{s}'_k)\right|^2 \leq 0, \quad \forall k \tag{28b}$$

$$\sum_{\upsilon\in\Delta} q_{k,\upsilon} \leq 1, \forall k \tag{28c}$$

$$\sum_{i\neq k}^{K} \left|\mathbf{g}_k^H(\mathbf{g}_i \odot \mathbf{s}'_i)\right|^2 \leq \text{LMUI}, \quad \forall k \tag{28d}$$

$$s'_t \leq P_k^{1/2}, \quad \forall k \tag{28e}$$

$$q_{kt} \in \{0,1\}, \quad \forall k. \tag{28f}$$

Note that this formulation consists in a power optimization of beam selection $\mathbf{s}'$ since it can assume any continue positive value limited to available total transmit power, i.e., $\sum_{kt} s_{t,k}^2 \leq P$.

In general, even with relaxation, the problem is complex to solve because it involves a joint optimization of discrete and continuous variables. In the next subsection, we present a heuristic based on Lagrangean relaxation for reducing the complexity of this MILP formulation.

4.3 | Lagrangean Relaxation via Dual Subgradient Optimization Algorithm

The idea follows the approach of the literature [3] to optimize the multi-UE precoder. The method aims to solve the MILP formulation (28) in the dual variable space [41], where the optimization problem becomes the unconstrained maximization of a non-differentiable concave function. Thus, a standard iterative subgradient descent method can be used to solve the corresponding dual problem.

The first step to find the dual version of the problem is to build the partial Lagrangean function $L(\mathbf{q}, \mathbf{s}', \lambda)$ by "relaxing"

(or "dualizing") the constraints (28b), that is, by adding these constraints to the MILP objective function (28a) weighted by the dual variables λ_k (i.e., the Lagrangean multipliers):

$$L(\mathbf{q}, \mathbf{s}', \lambda) = -\sum_{k}\sum_{\upsilon} \delta_\upsilon q_{k\upsilon} + \sum_{k} \lambda_k \left(\sum_{\upsilon\in\Delta} \gamma_{k\upsilon} q_{k\upsilon} A_k - \left| \mathbf{g}_k^H (\mathbf{g}_k \odot \mathbf{s}'_k) \right|^2 \right). \quad (29)$$

The minimization of the partial Lagrangean function $L(\mathbf{q}, \mathbf{s}', \lambda)$ constitutes the so-called Lagrangean relaxed version of the primal (30):

$$W(\lambda) = \min \; L(\mathbf{q}, \mathbf{s}', \lambda), \quad (30a)$$

$$\text{s.t.} \sum_{\upsilon\in\Delta} q_{k\upsilon} \leq 1, \quad \forall k, \quad (30b)$$

$$\sum_{i\neq k}^{K} \left| \mathbf{g}_k^H (\mathbf{g}_i \odot \mathbf{s}'_i) \right|^2 \leq \text{LMUI}, \quad \forall k, \quad (30c)$$

$$s'_t \leq P_k^{1/2}, \quad \forall k, \quad (30d)$$

where $W(\lambda)$ is the dual function, whose maximization comes up to the dual problem (31) to solve via the subgradient descent method:

$$\max_{\lambda} W(\lambda) \quad (31a)$$

$$\text{s.t. } \lambda \geq 0. \quad (31b)$$

The Lagrangean relaxed primal problem (30) can be separated into two independent subproblems, defined on a different groups of decision variables $\mathbf{q}$ and $\mathbf{s}'$, respectively, since the linking constraint (28b) between $\mathbf{q}$ and $\mathbf{s}'$ has been relaxed. The first subproblem (32) selects the UE-data rate assignment $\mathbf{q}$, while the second one (33) finds the optimized power beam associated to the UEs, represented by $\mathbf{s}'$.

$$\min_{\mathbf{q}} -\sum_{k}\sum_{\upsilon} \delta_\upsilon q_{k\upsilon} + \sum_{k} \lambda_k \left(\sum_{\upsilon\in\Delta} \gamma_{k\upsilon} q_{k\upsilon} A_k \right), \quad (32)$$

s.t. (30b).

$$\min_{\mathbf{s}'} -\sum_{k} \lambda_k \left| \mathbf{g}_k^H (\mathbf{g}_k \odot \mathbf{s}'_k) \right|^2, \quad (33)$$

s.t. (30c), (30d).

This decouple my results in two less complex subproblems than the original MILP problem. The power beam allocation subproblem (33) can be solved by well-known linear programming (LP) algorithms in polynomial time. On the other hand, the UE-data rate assignment subproblem (32) can be solved separately for each UE k, yielding to the next trivial solution (35):

$$w_{k\upsilon} = \delta_\upsilon - \lambda_k \gamma_{k\upsilon} A_k \quad (34)$$

$$q^\star_{k\upsilon} = \begin{cases} 1, \text{ if } \upsilon = \arg\max_{\{\upsilon\in\Delta | w_{k\upsilon}\geq 0\}} w_{k\upsilon} \\ 0, \text{ otherwise.} \end{cases} \quad (35)$$

Since, for each UE k, the set of values $w_{k\upsilon}$ are sorted by construction, this solution can be found by a standard binary search algorithm performing $\mathcal{O}(log_2(|\Delta|))$ comparisons.

The optimization of both LP subproblems parameterized by the current multipliers λ delivers a value for the dual function $W(\lambda)$ and a solution $\{\mathbf{q}^\star, \mathbf{s}'^\star\}$ to the Lagrangean relaxed primal problem. We must note that the UE-data rate assignment $\mathbf{q}$ could be unfeasible since we have relaxed the constraints (28b). Then, we build a feasible primal solution by keeping $\mathbf{s}'^\star$ and taking as feasible UE-data rate assignment $\mathbf{q}^{feas}$ the largest UE data rate supported by $\mathbf{s}'^\star$, i.e. meeting the constraints (28b), for each UE k. Afterwards, the method explores the dual solution space by using a subgradient update step to move from the current λ to a new set of values.

Since we know from (30) that the dual function is a convex function subject to the non-negativity constraints, represented by the vector λ, a descent step method used in unconstrained optimization is suitable for the dual exploration. In particular, a subgradient vector is used as search direction because the dual function is piecewise linear, and then non differentiable. This subgradient vector, ρ, is calculated as:

$$\rho = \nabla W(\lambda) = \sum_{\upsilon\in\Delta} \gamma_{k\upsilon} q_{k\upsilon} A_k - \left| \mathbf{g}_k^H (\mathbf{g}_k \odot \mathbf{s}'_k) \right|^2. \quad (36)$$

Then, the new λ in the dual space in the next iteration $l+1$ is updated by the subgradient step as:

$$\lambda^{l+1} = \max\{\lambda^l + \tau\rho, \mathbf{0}\}. \quad (37)$$

where τ is the fixed step size.

The new dual multipliers λ^{l+1} are replaced in the Lagrangean function (29), yielding to new instances of the Lagrangean relaxed subproblems (32) and (33) for the $(l+1)^{\text{th}}$ iteration. Then, after solving them, a new subgradient optimization step follows. The method continues by solving in an alternate way Lagrangean relaxed primal subproblems and dual problems at each iteration until a stopping criterion is met.

In this paper, the algorithm is stopped when any of the following conditions is satisfied first: (1) the *optimality* gap between the objective function (28a) evaluated for $\mathbf{q}^{feas}$ and the *upper bound* $\overline{W}$ diminishes under a threshold *thr*; (2), at least one Lagrange multiplier becomes null; or (3), a maximal number of iterations $l_{\max}$ is reached. The upper bound $\overline{W}$ is calculated as follows:

$$\overline{W} = \sum_{k=1}^{K} \log_2(1 + \text{SINR}_k^{UB}) \quad (38)$$

$$\text{SINR}_k^{UB} = \min\left(\left| \mathbf{g}_k^H (\mathbf{g}_k \odot \mathbf{s}'_k)^2 \right|, \gamma_{MAX} \right). \quad (39)$$

where $s'_t = P_k$ and γ_{MAX} is the largest SINR level allowed in the system (e.g, the value associated to the last index $\upsilon \in \Delta$ in Table 1). Finally, the rationale behind the second stopping criterion is related to the impact of the λ multipliers in

the Lagrangean relaxed primal subproblems. If λ_k becomes null, the subproblem (32) will assign the largest data rate available allowed in the the system to the UE k, whereas the subproblem (33) will allocate a null amount of power to UE k. That results is an abrupt transition in the λ_k evolution: from a smooth decreasing till reaching zero, we pass suddenly to a huge increment. In other words, the UE with the smallest impact on the objective function (the closest λ_k to zero) becomes presumably the UE with the highest impact. This change modifies drastically the solution $\mathbf{s}'^{\star}$ delivered by the subproblem (33), and, hence the feasible UE-data rate assignment $\mathbf{q}^{feas}$ built from $\mathbf{s}'^{\star}$ as aforementioned. The second stopping criterion prevents such situation.

4.4 | Low Complexity Heuristics

In some practical systems, it could be impossible to apply the last heuristic because its computational complexity becomes too high. Motivated by this fact, we propose three low-complexity heuristics to select the transmit beams. These heuristics are simple and less complex compared to the previous solutions in Section 4. Thereby, the performance results have improvements compared to the MRT case. In the following, the heuristics are presented.

4.4.1 | Heuristic 1 – Minimum-Interference Greedy Assignment

This heuristic tries to minimize interference (equivalently maximize SINR). Consider two UEs as an example. For each pair i, k of UEs, we maximize $\dfrac{\mathbf{g}_i^H \mathbf{s}_i + \mathbf{g}_k^H \mathbf{s}_k}{\mathbf{g}_i^H \mathbf{s}_k + \mathbf{g}_k^H \mathbf{s}_i}$. More specifically, this heuristic follows the steps:

1. Initialize with $\mathbf{s}_k = \mathbf{g}_k$;
2. For all pairs i, k of UEs, test all beams t. If removing $s_{t,k}$ leads to a higher SINR, turn this to 0.

The idea is to minimize the interference and, under this perspective, this heuristic marginally improves the SINR, compared to the simple MRT approach. This heuristic is more formally described by the pseudo-code presented in Algorithm 1.

4.4.2 | Heuristic 2 – Munkres-based Assignment

Inspired again by the MRT scheme, we consider in this proposed heuristic that each UE will get assigned only one beam, which will concentrate the whole power allocated to that UE, and that each beam will be assigned to at most one UE. Since we are concerned with the overall performance of the K UEs, we can consider the following alternative optimization problem:

$$\mathbf{S}^{\star} = \arg\max_{\mathbf{S}} \{\mathbf{1}_{M_T}^T (\mathbf{G} \odot \mathbf{S}) \mathbf{1}_K\}, \tag{40a}$$

$$\text{s.t. } \mathbf{S}\mathbf{1}_K = \mathbf{1}_K, \quad \mathbf{1}_{M_T}^T \mathbf{S} \leq \mathbf{1}_{M_T}^T, \quad \mathbf{S} \in \mathbb{B}^{M_T \times K}, \tag{40b}$$

which implies that each UE will be assigned a single beam and each beam will be assigned to a single UE. The above assignment problem corresponds to a maximum matching in a bipartite graph and can be solved optimally using Munkres' algorithm[23] (see Algorithm 2). Due to the limited space, we omit the details of the Munkres' algorithm.

In spite of involving the solution of an optimization problem, the Munkres' algorithm solves the assignment problem with $\mathcal{O}\left(\min\left\{K^3, M_T^3\right\}\right)$ complexity[23]. Notice that, whenever there are more beams than UEs, the output of this heuristic could be augmented by assigning additional beams to the UE.

Algorithm 1 Minimum-Interference Greedy Assignment

Input : A $\mathbf{G}^H$ matrix of size $K \times M_T$
Output: An $\mathbf{S}$ matrix of size $K \times M_T$

Initialize $\mathbf{S} = \mathbf{G}$
Define the interference limit $\mathbf{g}_i^H \mathbf{s}_k + \mathbf{g}_k^H \mathbf{s}_i$
while *Exist an UE that violates the interference limit* **do**
  Remove the beam of the UE
  Re-evaluate the limit
end

Algorithm 2 Munkres-based Assignment

Input : A $\mathbf{G}^H$ matrix of size $K \times M_T$
Output: An $\mathbf{S}$ matrix of size $K \times M_T$

Define $\mathbf{G}'$ *so that* $g'_{i,j} = 1/g_{i,j}$
$\mathbf{S} \leftarrow$ *munkres*$(\mathbf{G}')$

4.4.3 | Heuristic 3 – Minimum Interference Greedy Assignment with Munkres Initialization

Based on the previous heuristic, one can consider augmenting the obtained solution by assigning new beams to the UE whenever it does not compromise the overall performance. In this case, a slightly modified heuristic could be applied which combines aspects of the two previous heuristics. Denoting by $\mathcal{B}_i$ the set of beams assigned to UE i and by $\mathcal{K}_t$ the set of UEs using the beam t, the heuristic is described as follows. We assume in Algorithm 3 that the unsatisfied UE are those whose minimum SINR requirement is not satisfied.

Algorithm 3 Minimum-Interference with Munkres Initialization

Input : A $\mathbf{G}^H$ matrix of size $K \times M_T$
Output: An $\mathbf{S}$ matrix of size $K \times M_T$

Define $\mathbf{G}'$ *so that* $g'_{i,j} = 1/g_{i,j}$
$\mathbf{S} \leftarrow$ *munkres*$(\mathbf{G}')$
while *there is no unsatisfied UE* **do**
  Select the scheduled UE i *and the beam* $t \notin \mathcal{B}_i$ *with highest ratio* $\dfrac{\mathbf{g}_i^H \sum_{t' \in \mathcal{B}_i} s_{t',i} + \mathbf{g}_i^H s_{t,i}}{\max_{i' \in \mathcal{K}_i} \{0,\ \mathbf{g}_{i'}^H s_{t,i'}\}}$
  if *all UEs are satisified when assigning beam* t *to UE* i **then**
    Allocate beam t *to UE* i
  else
    Break
  end
end

The basic idea behind the above heuristic is to allocate a new beam to the UE such that the gain is maximized and that the interference (from the worst interferer) is minimized.

After the beam selection/assignment step, power allocation among UEs is performed along the lines[3].

5 | SIMULATIONS RESULTS

In this section, we compare the performance of linear precoders as well as the schemes based on heuristics and the corresponding optimal solution provided by the MILP formulation described in (3). The power allocation per UE applied in Heuristics 1, 2, 3, ZFBF and MRT can be reproduced following the supplementary material[3].

We assume a system with $M_T = 64$ antennas and scenarios with different sparsity levels. For all simulations, we ensure that the sparsity level is less than or equal to χ. The curves are plotted as a function of the signal-to-noise ratio (SNR) $\left|\mathbf{H}_k^H \mathbf{w}_k\right|^2 / \sigma_k^2$ and the average sum rate is described by (16). Following (21), the SINR of the k^{th} UE achieves the best performance when the LMUI is equal zero. Therefore, we present the best solutions with the best beam selection in the interference-free case.

In all simulations, we use 1000 channel realizations. In the simulation results we assume the two channel models presented in section 2: one is called i.i.d. and the other is a geometric-stochastic channel, both with the same specified sparsity level χ. In the i.i.d. channel model the elements of $\mathbf{g}$ follow a zero-mean circularly symmetric complex Gaussian distribution, $\mathbf{g}_k \in \mathcal{CN}(0, \mathbf{I}_{M_T})$ following (8). In the geometric-stochastic channel, each element in $\mathbf{G}$ was generated according to (10). In this model, we generate the channel removing the smallest elements in $\mathbf{g}_k$ until reaching a required sparsity level χ. We consider $L = 20$ scatterers[42], which are enough to capture the channel characteristics. As for the optimal solutions, we solve (28) (i.e., the MILP problem) and the Lagrangean relaxation (LA) described in Section 4.3 using the CPLEX solver[43]. For the Lagrangean, we assume $\tau = 10^{-6}$ and $l_{max} = 1000$.

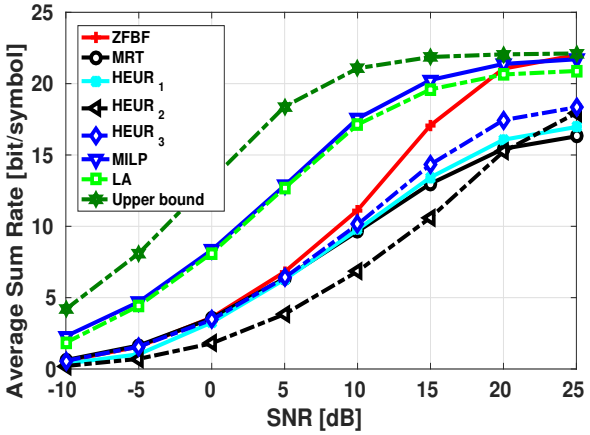

(a) Performance using an i.i.d. channel model.

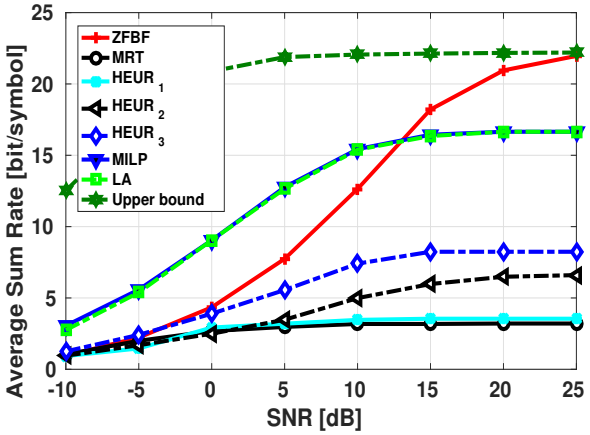

(b) Performance using the geometric-sthocastic channel model.

FIGURE 2 Performance of optimal solution (MILP), Lagrangean relaxation, ZFBF, MRT and three proposed heuristics with $K = 4, M_T = 64$ and sparsity level equal to 90%.

Figure 2 (a) shows the performance results under the parameters of Table 1 . Note that the performances of all schemes are upper limited at 22 bits per symbol, since the data in Table 1 restricts the problem to assign at most the rate of 5.5 bits/symbol per UE, ($\Delta \in [0.15,\ 5.5]$). Then, in the solutions, the maximum sum rate is $K \cdot 5.5 = 22$ bits per symbol.

The improved results of our proposal compared to ZFBF comes from a better management of beam power in the beam domain, whereas in the second step (i.e., the UE power optimization), the heuristic for ZFBF distributes equally the power among all non-zero beams of each UE. Besides that, ZFBF "wastes" power in the process of eliminating interference (ill-conditioning) (see Figure 5). However, when the sparsity level is decreased (more non-zero elements), the ZFBF can increase the performance (better conditioning), as we can see in Figure 6 . Different from MILP and LA simulation results, in the low-complexity heuristics we consider a beam selection followed by UE power optimization[3]. The ZFBF and MRT follow with the same power optimization.

Considering the low-complexity heuristics, MRT and ZFBF, in the low SINR, MRT and heuristic 2 are good options since MUI is not dominant and the heuristics have low complexity with similar performance. In the medium and high SINR ranges, the performance of MRT is limited by MUI. In this case, the knowledge about the beams exploited by the proposed heuristic leads to improvements in the sum rate. The heuristic 1 is based on MRT and hence, using knowledge about the beams improves the rate. In heuristic 2, the allocation of just one beam per UE has low performance in the low SINR. However, under high SINRs the performance is increased since the K beams are interference-free. The result of heuristic 3 is similar to that of MRT and heuristic 1 for low SINR. However, for medium and high SINR values the performance has improved compared to the MRT because of the potential addition of extra beams to each UE.

In Figure 2 (b) we evaluate the proposal considering the stochastic-geometric channel model in Section 2.3. Note that the ZFBF has similar performance since it is able to eliminate the MUI in any scenario. However, MRT loses performance. Hence, the heuristics performance is affected, since we have more interfering beams, reducing the overall performance. One reasonable explanation for this behavior is that in the stochastic-geometric channel the accuracy of the model is better than that of the i.i.d. channel model, thus capturing the interference among beams more effectively. While in the i.i.d. channel model the geometry of interference follows a Bernoulli distribution.

Note that the Lagrangean relaxation can achieve the maximum performance of the MILP for almost all SNRs values. The upper bound curve is achieved by (38), and the thr (gap) is adapted for each SNR. For low SNR values, we use higher values for thr. Otherwise, for high SNR values, we use lower values for thr since the gap between the MILP and upper bound solution is smaller. Thus, we adapt the threshold values to ensure a small number of iterations for achieving the MILP solution. Note that the value of thr for each channel model can be set differently. The average number of iterations

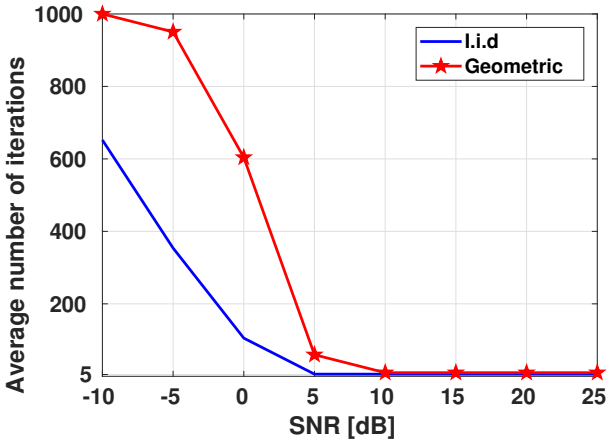

FIGURE 3 Average number of iteration for the Lagrangean convergence.

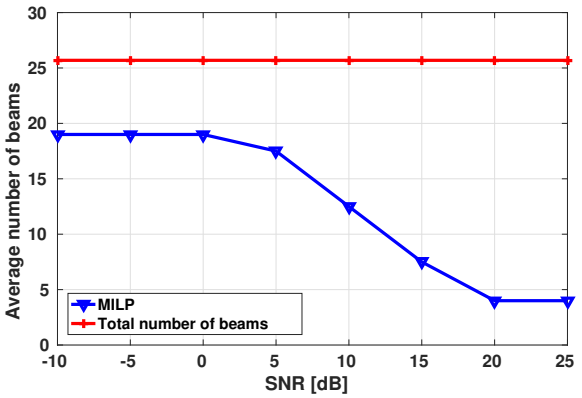

FIGURE 4 Average number of selected beams for $K = 4$.

is shown in Figure 3 . Note that a low number of iterations is sufficient to reach a good convergence. For the i.i.d. channel model, $thr = 0.4$ is chosen to reach a MILP solution. For the geometric-stochastic channel model, $thr = 0.5$ for low SNR values, and for high SNR values, $thr = 0.25$, are chosen to achieve MILP solutions.

In the optimal solution for beam selection, some beams are not used. Therefore, the "less is more" principle[44] (c.f. Figure 3.8 - Chapter 3) that usually plays an important role in ZFBF takes effect, i.e., fewer beams with more power lead to a better allocation. In Figure 4 , we present the optimal average number of selected beams according to the MILP solution and the average number of total beams with sparsity level $\chi = 90\%$. In general, in this interference-free solution, when more power can be allocated, the MILP solution reduces the number of beams to be equal to the number of UE.

Figure 5 illustrates an example of beam selection and power optimization for a SNR $= -10$ dB and shows 2 UEs.

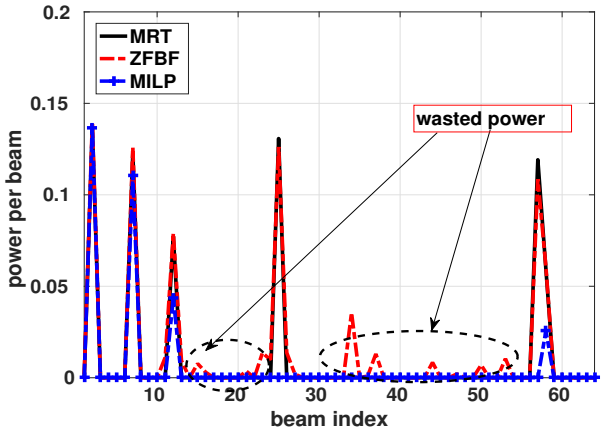

(a) UE-1

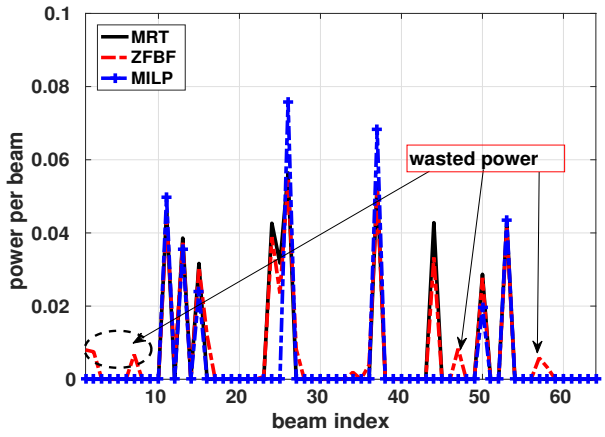

(b) UE- 2

FIGURE 5 Illustrative example for beams selection and power optimization using MILP, ZFBF and MRT.

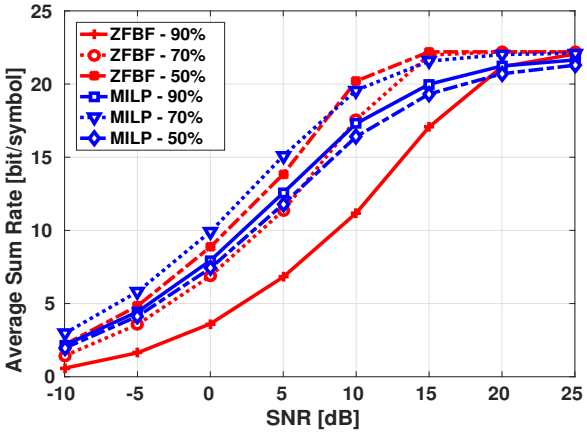

(a) With Table 1 values using the i.i.d. channel model.

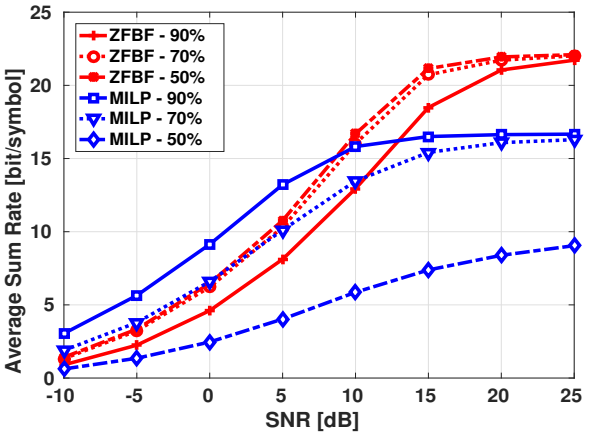

(b) With Table 1 values using the geometric-sthocastic channel model.

FIGURE 6 Comparative performance of MILP and ZFBF with different sparsity levels for $K = 4$ and channel models.

The reduction of beam number is recognized where some of them are not used, compared to the MRT, which uses all beams, and to the solution MILP. Note that in some cases power is allocated where there are no beams for the ZFBF. It happens because ZFBF eliminates all interference beams. Thereby, part of the power is wasted out in the process.

Figure 6 (a) illustrates MILP and the performance of ZFBF with the i.i.d. channel for sparsity level χ equal to 90%, 70% and 50% and for $K = 4$. When the sparsity level has decreased, the ZFBF performance is increased. The best solution for our proposal is found with $\chi = 70\%$. Figure 6 (b) considers the geometric-stochastic channel. The best solution is found with $\chi = 90\%$. When the sparsity level is decreased, the performance of the MILP solution is decreased. When the level of the sparsity of $\mathbf{G}$ is decreased, there is more interference, and the performance degrades. The ZFBF performance is increased with the decreasing of sparsity levels for both channel models.

5.1 | Heuristics Robustness

In order to evaluate the performance and robustness of the proposed heuristics in a practical scenario, we consider a controlled error in the CSI. The imperfect CSI is modeled as $\hat{\mathbf{G}} = \mathbf{G} + \mathbf{E}$, where $\mathbf{E} \approx \mathbb{CN}(0, \sigma_e^2)$. In Figure 7 , we present the results for the average sum rate with the channel $\chi = 90\%$ and $K = 4$. In these simulations we considered several σ_e^2 values and we have observed in our simulation results that the performance is similar for different small values of σ_e^2. Furthermore, we show the results for $\sigma_e^2 = 0.5$ in which the performance losses are smaller compared to the perfect CSI. Thereby, as for the MRT, the heuristics are robust to the error. All heuristics have small performance losses in both channel models.

In general, the channel estimator can reach an estimate with precision more than 0.1. Thus, the proposed heuristics have shown a good robustness to imperfect channel knowledge.

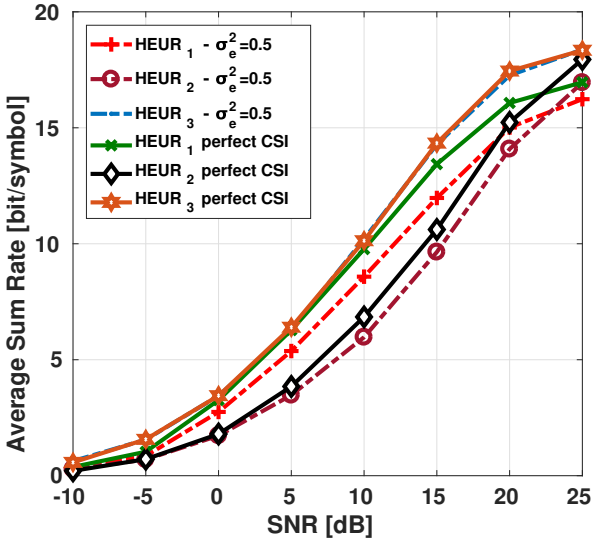

(a) Imperfect CSI using i.i.d. channel model.

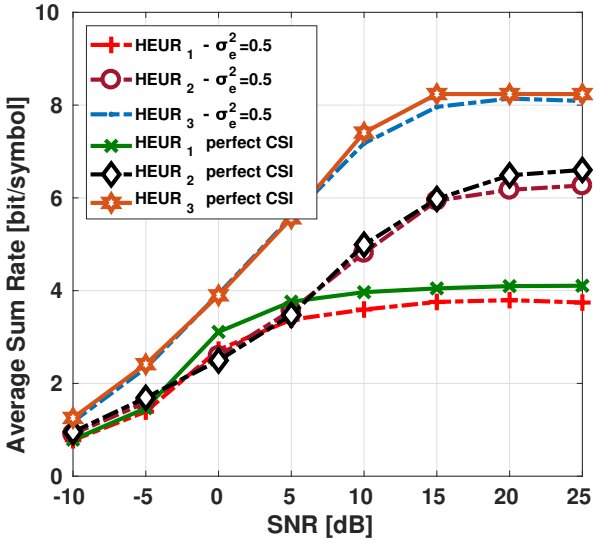

(b) Imperfect CSI with geometric-stochastic channel model.

FIGURE 7 Performance of three proposed heuristics to $K = 4$, $M_T = 64$ with $\chi = 90\%$.

5.2 | Complexity Analysis

The computational complexity gives an upper bound on the computational resources required by an algorithm and is represented by the asymptotic notation $\mathcal{O}(\cdot)$. LP problems are usually solved by *Active Set Methods*, where the Simplex Method is the standard approach, or by *Interior Point Methods*[45]. In our case, CPLEX[43] reports the use of dual version of the Simplex algorithm to solve all the LP problems presented in this paper. Simplex complexity can be computed as the product of the number of Simplex iterations by the number of elementary operations at each iteration (that is exactly of $\mathcal{O}(mn)$, where n is the number of variables and m is the number of constraints in the *Standard Form* of a LP problem). On the other hand, the number of Simplex iterations has an exponential crude bound of $\mathcal{O}(n^m)$[46,47], but in most of the practical cases this bound is $\mathcal{O}(m+n)$[45]. When $m \ll n$ in the primal version of a LP, the number of variables and constraints in the *Standard Form* of the dual version becomes close to n, allowing estimating a practical upper bound on the Simplex Complexity of $\mathcal{O}\left(n^3\right)$. That is the case of our LP problems since $K \ll M_T$, and then, $m \ll n$. For the case of a MILP problem, like the problem (28), the CPLEX solver uses the branch-and-bound (BnB) algorithm. For an arbitrary number of discrete variables n_d, the number of LP subproblems of $\mathcal{O}\left(n^3\right)$ to be solved is at least $(\sqrt{2})^{n_d}$[40], yielding to a total complexity estimation of $\mathcal{O}\left((\sqrt{2})^{K|\Delta|} \cdot (K|\Delta| + KM_T)^3\right)$, for the problem (28). In the Lagrangean approach, the solution is reached solving l iterations for the two LP Lagrangean Relaxed subproblems (32) and (33). The first one can be solved by K binary searches of complexity $\mathcal{O}(log_2(|\Delta|))$, meanwhile the second one is solved by a Dual Simplex with a complexity of $\mathcal{O}\left(n^3\right) = \mathcal{O}\left(K^3 M_T^3\right)$ as indicated before. Assuming that $K \ll M_T$ in the massive MIMO case, the complexity of MILP, Lagrangean, precoders and heuristics can be expressed as in Table 2 .

TABLE 2 Complexity evaluation.

Solution	Complexity
ψ_{MILP}	$\mathcal{O}\left((\sqrt{2})^{K\|\Delta\|} \cdot (K\|\Delta\| + KM_T)^3\right)$
$\psi_{Lagrangean}$	$\mathcal{O}\left(l \cdot (Klog_2(\|\Delta\|) + K^3 M_T^3)\right)$
ψ_{MRT}	$\mathcal{O}\left(KM_T\right)$
ψ_{ZFBF}	$\mathcal{O}\left(K^2 M_T^2\right)$
ψ_{HEUR_1}	$\mathcal{O}\left(KM_T\right) + \mathcal{O}\left(K^2 M_T\right)$
ψ_{HEUR_2}	$\mathcal{O}\left(\min\left\{K^3, M_T^3\right\}\right)$
ψ_{HEUR_3}	$\mathcal{O}\left(\min\left\{K^3, M_T^3\right\}\right) + \mathcal{O}\left(KM_T\right)$

In the MILP formulation, $(\sqrt{2})^{K|\Delta|}$ LP subproblems are solved with polynomial complexity on $|\Delta|$, K and M_T, while in the Lagrangean approach, l less complex LP subproblems are solved with sub-linear complexity on $|\Delta|$ and polynomial on K and M_T. Moreover, this number of l problems does not depend on the size problem (K and $|\Delta|$) as the MILP case, but the method accuracy ϵ, that is, the absolute optimality gap, since the Lagrangean approach is a subgradient method whose worst-case complexity is $\mathcal{O}\left(1/\epsilon^2\right)$ iterations[48]. Then, fixing an arbitrary ϵ, we can bound the Lagrangean complexity, in contrast to the MILP formulation.

The complexity of heuristic 1 (ψ_{HEUR_1}) is basically the MRT with the addition of the beam selection complexity

$\mathcal{O}\left(K^2 M_T\right)$. The complexity of heuristic 2 (ψ_{HEUR_2}) is low because the algorithm finds one beam per UE. Heuristic 3 combines the complexity of heuristic 2 (ψ_{HEUR_2}) and the complexity of beams searching for additional beams. Therefore, heuristics 1 and 3 are more complex than MRT due to the additional complexity in selecting extra beams. However, they are less complex than ψ_{ZFBF}. The heuristic 2 is less complex compared to MRT, however it is only suitable for high SNR and sparsity levels.

Comparing the optimal solution given by MILP or Lagrangean relaxation, the performance of proposed heuristics have low performance. However, this loss in performance is explained by significant reduction of complexity.

6 | CONCLUSIONS

In this paper, we have formulated a precoder design using two different sparse beam channel models. We have shown the best solution for MRT with selection and proposed three simple heuristics to select the beams in a massive-BS MU scenario.

The proposed heuristics have a good performance under high sparsity levels compared to the MRT precoder, and we show that beam selection improves the system performance with low-complexity.

Furthermore, we have given the optimal solution to select the beams, assign the data rates and the transmit powers to MU for a practical system using the LTE table. We have proposed a less complex heuristic using Lagrangean relaxation and have shown that the proposed approach is closed to optimal.

ACKNOWLEDGMENTS

This work was realized with support of CNPq (Conselho Nacional de Desenvolvimento Científico e Tecnológico - Brazil).

References

1. Larsson E. G., Edfors O., Tufvesson F., Marzetta T. L.. Massive MIMO for Next Generation Wireless Systems. *IEEE Communications Magazine.* 2014;52(2):186-195.

2. Marzetta T. L.. Noncooperative Cellular Wireless with Unlimited Numbers of Base Station Antennas. *IEEE Transactions on Wireless Communications.* 2010;9(11):3590-3600.

3. Björnson E., Bengtsson M., Ottersten B. E.. Optimal Multiuser Transmit Beamforming: A Difficult Problem with a Simple Solution Structure [Lecture Notes]. *IEEE Signal Processing Magazine.* 2014;31(4):142–148.

4. Gershman A. B., Sidiropoulos N. D., Shahbazpanahi S., Bengtsson M., Ottersten B.. Convex Optimization-Based Beamforming. *IEEE Signal Processing Magazine.* 2010;27(3):62-75.

5. Rashid-Farrokhi F., Liu K. J. R., Tassiulas L.. Transmit eamforming and power control for cellular wireless systems. *IEEE Journal on Selected Areas in Communications.* 1998;16(8):1437-1450.

6. Bengtsson M., Ottersten B.. Optimal and Suboptimal Transmit Beamforming. In: Handbook of Antennas in Wireless Communications. CRC Press 2001 (pp. 18–1).

7. Kerret P., Gesbert D.. Sparse Precoding in Multicell MIMO Systems. In: IEEE Wireless Communications and Networking Conference (WCNC):958-962; 2012.

8. Sun C., Gao X., Jin S., Matthaiou M., Ding Z., Xiao C.. Beam Division Multiple Access Transmission for Massive MIMO Communications. *IEEE Transactions on Communications.* 2015;63(6):2170–2184.

9. Yu Y., Wang P., Chen H., Li Y., Vucetic B.. A Low-Complexity Transceiver Design in Sparse Multipath Massive MIMO Channels. *IEEE Signal Processing Letters.* 2016;23(10):1301-1305.

10. Li L., Ashikhmin A. E., Marzetta T. L.. Interference Reduction in Multi-Cell Massive MIMO Systems II: Downlink Analysis for a Finite Number of Antennas. *Computing Research Repository (CoRR).* 2014;abs/1411.4183.

11. Cheng Y., Pesavento M.. Joint Discrete Rate Adaptation and Downlink Beamforming Using Mixed Integer Conic Programming. *IEEE Transaction Signal Processing.* 2015;63(7):1750–1764.

12. Weichselberger W., Herdin M., Ozcelik H., Bonek E.. A Stochastic MIMO Channel Model with Joint Correlation of Both Link Ends. *IEEE Transactions Wireless Communications.* 2006;5(1):90–100.

13. Bajwa W. U., Haupt J., Sayeed A. M., Nowak R.. Compressed Channel Sensing: A New Approach to Estimating Sparse Multipath Channels. *Proceedings of the IEEE.* 2010;98(6):1058–1076.

14. Holma H., Toskala A.. *LTE for UMTS - OFDMA and SC-FDMA Based Radio Access*. Wiley Publishing; 2009.

15. Yu Y., Wang P., Chen H., Li Y., Vucetic B.. A Low-Complexity Transceiver Design in Sparse Multipath Massive MIMO Channels. *IEEE Signal Processing Letters.* 2016;23(10):1301-1305.

16. Sayeed A., Brady J.. Beamspace MIMO for High-Dimensional Multiuser Communication at Millimeter-Wave Frequencies. In: 2013 IEEE Global Communications Conference (GLOBECOM):3679-3684; 2013.

17. Hogan J., Sayeed A.. Beam Selection for Performance-Complexity Optimization in High-Dimensional MIMO Systems. In: 2016 Annual Conference on Information Science and Systems (CISS):337-342; 2016.

18. Rappaport T. S., Sun S., Mayzus R., et al. Millimeter Wave Mobile Communications for 5G Cellular: It Will Work!. *IEEE Access.* 2013;1:335-349.

19. Kolomvakis N., Matthaiou M., Coldrey M.. Massive MIMO in Sparse Channels. In: 2014 IEEE International Workshop on Signal Processing Advances in Wireless Communications (SPAWC), Toronto, ON, Canada:21–25; 2014.

20. Barbotin Y., Hormati A., Rangan S., Vetterli M.. Estimation of Sparse MIMO Channels with Common Support. *IEEE Transactions on Communications.* 2012;60(12):3705–3716.

21. Xie H., Gao F., Jin S.. An Overview of Low-Rank Channel Estimation for Massive MIMO Systems. *IEEE Access.* 2016;4:7313–7321.

22. Corbillon X., A-.Pardo R., Kuhn N., Texier G., Simon G.. Cross-Layer Scheduler for Video Streaming over MPTCP. In: Proceedings of the 7th International Conference on Multimedia Systems (MMSys):7:1–7:12; 2016.

23. Kuhn Harold W.. The Hungarian Method for the Assignment Problem. In: 50 Years of Integer Programming 1958-2008 - From the Early Years to the State-of-the-Art. Springer 2010 (pp. 29–47).

24. Valduga S. T., Deneire L., De Almeida A. L. F., Maciel T. F., A-.Pardo R.. Low Complexity Beam Selection for Sparse Massive MIMO Systems. In: International Symposium on Wireless Communication Systems (ISWCS); 2017; Bologna, Italy.

25. Bajwa W.U., Sayeed A., Nowak R.. Sparse Multipath Channels: Modeling and Estimation. In: Digital Signal Processing Workshop and 5th IEEE Signal Processing Education Workshop, 2009. DSP/SPE 2009:320-325; 2009.

26. Cai W., Wang P., Li Y., Zhang Y., Pan P.. Asymptotic Capacity Analysis for Sparse Multipath Multiple-Input Multiple-Output Channels. *IEEE Communications Letters.* 2015;19(12):2262-2265.

27. Adhikary A., Nam J., Ahn J. Y., Caire G.. Joint Spatial Division and Multiplexing - The Large-Scale Array Regime. *IEEE Transaction Information Theory.* 2013;59(10):6441–6463.

28. Song G. H., Brady J., Sayeed A.. Beamspace MIMO Transceivers for Low-Complexity and Near-Optimal Communication at mm-Wave Frequencies. In: 2013 IEEE International Conference on Acoustics, Speech and Signal Processing (ICASSP):4394-4398; 2013.

29. Brady J., Sayeed A.. Beamspace MU-MIMO for high-density gigabit small cell access at millimeter-wave frequencies. In: 2014 IEEE 15th International Workshop on Signal Processing Advances in Wireless Communications (SPAWC):80-84; 2014.

30. Björnson E., Jorswieck E. A.. Optimal Resource Allocation in Coordinated Multi-Cell Systems. *Foundations and Trends in Communications and Information Theory.* 2013;9(2-3):113–381.

31. Liu Y. F., Dai Y. H., Luo Z. Q.. Coordinated Beamforming for MISO Interference Channel: Complexity Analysis and Efficient Algorithms. *IEEE Transaction on Signal Processing.* 2011;59(3):1142–1157.

32. Yang H., Marzetta T. L.. Performance of Conjugate and Zero-Forcing Beamforming in Large-Scale Antenna Systems. *IEEE Journal on Selected Areas in Communications.* 2013;31(2):172–179.

33. Ashikhmin A. E., Marzetta T. L., Li L.. Interference Reduction in Multi-Cell Massive MIMO Systems I: Large-Scale Fading Precoding and Decoding. *Computing Research Repository (CoRR).* 2014;abs/1411.4182.

34. Rusek F., Persson D., Lau B. K., et al. Scaling Up MIMO: Opportunities and Challenges with Very Large Arrays. *IEEE Signal Processing Magazine.* 2013;30(1):40-60.

35. Xu Y., Le-Ngoc T.. Global D.C. Optimization for Multi-User Interference Systems. In: 2nd IEEE International Workshop on Computational Advances in Multi-Sensor Adaptive Processing (CAMSAP):209-212; 2007.

36. Mohammed S. K., Larsson E. G.. Per-Antenna Constant Envelope Precoding for Large Multi-User MIMO Systems. *IEEE Transactions on Communications.* 2013;61(3):1059-1071.

37. Liu F., Masouros C., Amadori P. V., Sun H.. An Efficient Manifold Algorithm for Constructive Interference Based Constant Envelope Precoding. *IEEE Signal Processing Letters.* 2017;24(10):1542-1546.

38. Wai H. T., Li Q., Ma W. K.. A convex Approximation Method for Multiuser MISO Sum Rate Maximization under Discrete Rate Constraints. In: 2013 IEEE International Conference on Acoustics, Speech and Signal Processing (ICASSP):4759-4763; 2013.

39. Pang J. S., Scutari G., Palomar D. P., Facchinei F.. Design of Cognitive Radio Systems under Temperature-Interference Constraints: A Variational Inequality Approach. *IEEE Transactions on Signal Processing.* 2010;58(6):3251–3271.

40. Sierksma G.. *Linear and Integer Programming: Theory and Practice;*. Advances in applied mathematicsLondon: CRC Press; 2nd ed.2001.

41. Palomar D. P., Chiang M.. A Tutorial on Decomposition Methods for Network Utility Maximization. *IEEE Journal on Selected Areas in Communications.* 2006;24(8):1439-1451.

42. Meredith J. M., Krause J.. *Technical report (TR): Study on channel model for frequencies from 0.5 to 100 GHz.* 38.901: 3GPP; 2017.

43. IBM ILOG CPLEX Optimize http://www-01.ibm.com/software/integration/optimization/cplex-optimizer/2017.

44. Bartolomé D.. *Fairness Analysis of Wireless Beamforming Schedulers.* 2005.

45. Gondzio J.. Interior Point Methods 25 Years Later. *European Journal of Operational Research.* 2012;218(3):587–601.

46. Megiddo N.. Linear Programming in Linear Time When the Dimension Is Fixed. *Jornal of the ACM (JACM).* 1984;31(1):114–127.

47. RinnooyKan A.H.G., Telgen J.. The Complexity of Linear Programming. *Statistica Neerlandica.* 1981;35(2):91–107.

48. Shor N. Z., Kiwiel Krzysztof C., Ruszcayǹski Andrzej. *Minimization Methods for Non-differentiable Functions*. New York, NY, USA: Springer-Verlag New York, Inc.; 1985.